A regularization strategy for inverse source problems with applications in optics

J. A. Acevedo Vázquez[a], J. J. Oliveros Oliveros[a], J. J. Conde Mones[a] and M. M. Morín Castillo[b].

[a]*Facultad de Ciencias Físico Matemáticas, Benemérita Universidad Autónoma de Puebla, Avenida San Claudio y 18 Sur, Colonia San Manuel, Ciudad Universitaria, 72570, Puebla, México.*

[b]*Facultad de Ciencias de la Electrónica, Benemérita Universidad Autónoma de Puebla, Avenida San Claudio y 18 Sur, Colonia San Manuel, Puebla, 72570, Puebla, México.*

Received 16 November 2024; accepted 27 March 2025

In this work, we provide a stable algorithm for the inverse source problem where the region corresponds with a circle centered on the origin. The algorithm is obtained using an operational equation, which is ill-posed in the Hadamard sense due to the following points: firstly, many sources produce the same measurement and, secondly, due to the presence of numerical instability. If the operational equation is restricted to the Hilbert space of harmonic functions, the inverse source problem's uniqueness is guaranteed. The algorithm considers two regularization parameters to handle the numerical instability: the Tikhonov regularization parameter and the term N, where the series expansion is truncated. To illustrate the proposed algorithm, we developed one numerical example. Furthermore, we apply the algorithm to solve one inverse optical problem associated with the Intensity Transport Equation when the intensity distribution is considered almost uniform for the case in which the wavefront, which propagates in the direction of the optical axis, is considered within the paraxial approximation. The case where the source is not harmonic has no unique solution without a priori information. This work presents the case where the source belongs to functions that take two values. For this type, it is possible to recover the source completely. We give examples of the same application considering two cases for the source of the right side of the Intensity Transport Equation: when the source is a harmonic function and when it belongs to the above-mentioned type.

Keywords: Inverse source problem; ill-posed problem; regularization; irradiance transport equation; wavefront.

DOI: https://doi.org/10.31349/RevMexFis.71.050701

1. Introduction

Source identification problems are widely studied in many research fields, such as tomography, geophysics, inverse electrocardiography, inverse electroencephalography, industrial processes, etc. The inverse source identification problems determine the sources that produce a given measurement recorded on the region's boundary. These inverse problems are ill-posed in the Hadamard sense due to the following two points: many sources can produce the same measurement, and the problem of source recovering presents a numerical instability, i.e., small changes in the measurement can produce substantial variations in the sought source. Regularization techniques must be applied to handle this instability. In particular, we consider the Tikhonov regularization, which depends on a parameter that must be chosen in terms of the measurement's error. The forward problem is associated with the inverse problem, which consists of determining the measurements when the source is known. As the first step in studying inverse problems, the forward problem is studied since we get information on both the uniqueness of the solution and numerical instability. Furthermore, some inverse problems can be expressed as an operational equation of the form $Ax = y$, and the study of the forward and inverse problems can be done by considering the properties of the operator A. More precisely, an operational equation $Ax = y$ is well-posed if ([1])

1. A solution to the problem exists (existence).
2. There is at most one solution to the problem (uniqueness).
3. The solution depends continuously on the data (stability).

A problem is well-posed in modern language if the operator A is bijective and bicontinuous. A problem is ill-posed if it is not well-posed. In particular, when the operator A^{-1} is not continuous, numerical instability is present. Small changes in the measurement (right side of the equation) are inherent in the measurement devices. We emphasize that many application problems can be written as operational equations with operators whose inverses are not continuous.

This work considers the inverse source problem defined in a circular region. The relationships between the sources and measurements are established by an elliptic boundary value problem. Considering the geometry, the circular harmonics are used to express the sources, the solution of the boundary value problem, and the measurements. We get the regularized solution solving the normal equations from where we proposed the algorithm, which considers two parameters to handle the numerical instability: the Tikhonov regularization parameter and a parameter associated with a cut-off of the series used to represent the source, potentials, and measurements. In this work, we have the following original results:

- A regularization strategy, which depends on two parameters. First, it is the Tikhonov regularization pa-

rameter. Second, it is the parameter associated with the truncation of the series in which the source and measurement are expanded. This strategy (Algorithm 1) can be applied to recover harmonic sources defined in Ω.

- Algorithm 2 allows us to recover sources different to zero in a closed subset of Ω or the case in which the source depends on a finite number of parameters. From the measurement on $\partial\Omega$, we recover the harmonic component using Algorithm 1. Then, we define some functionals to recover the source completely, *i.e.*, the non-harmonic component of the source is recovered, considering prior information about the total source. Inverse source problems, it is usually considered apriori information about the source since those inverse problems are ill-posed in the Hadamard sense. That information about the source can be obtained from the knowledge of the studied problem, which guarantees uniqueness and finds stable algorithms to recover the sought source.

  In [2] the author considers the following:

  - The source $f \in L_2(\Omega)$ has compact support (the set of points where the function is not zero is closed and bounded) in a subdomain Ω^*, which is contained in the region Ω where the problem is studied.
  - The source f is piecewise constant.

  In [3], the authors consider the following:

  - The source has the form:

    $$f(x_1, x_2) = \varphi_1(x_2)g_1(x_1) + \varphi_2(x_2)g_2(x_1).$$

  - For the first step, they supposed that the functions g_1 and g_2 are known.
  - Then, they proposed an iterative algorithm for the general case.
  - They consider the full data on the boundary, *i.e.*, they do not consider the case of a finite number of points in which the measurement is taken.

  Other examples of these points can be found in Refs. [4–7]. The assumptions correspond to information about the sources. In this work, we follow this idea and consider two cases for the sources:

  - Harmonic sources in Ω.
  - Sources that are different from zero in a closed and bounded subset (compact) of Ω or the case in which the source depends on a finite number of parameters.

- Original synthetic examples were developed to show the feasibility of the proposed Algorithms.
- Original MATLAB programs were specifically developed to implement and execute Algorithms 1 and 2 efficiently. These programs are designed to consider the two key parameters in the regularization strategy proposed (Algorithm 1), ensuring accurate computation and reliable results. Also, Algorithm 2 is implemented *fmincon* routine to find the maximum of the approximated harmonic component on $\partial\Omega$, with a tolerance of 10^{-14}.
- The application to the following inverse optical problem:

  To find the irradiance from the wavefront measurement on the boundary of one circular region if the intensity distribution is considered to be almost uniform. Algorithms 1 and 2 were applied to solve, in stable form, this inverse problem.

  According to [8], there is a considerable amount of work to get the wavefront, but there is none for the inverse problem of finding the intensity from the wavefront. In that work, the authors used the ray counting method to get some values of the wavefront and then applied one discretization of the Laplace operator to find the irradiance. This work provides another approach.

In summary, this work gives a stable algorithm that considers two regularization parameters for the inverse source problem defined in a circular region centered in the origin.

This work is divided as follows: In Sec. 1, the Introduction provides the basic ideas, among which we can find the ill-posedness of the inverse source problem studied. Also, an optical application is presented. In Sec. 2 presents the mathematical model used to find an operational equation acting between Hilbert spaces, which allows us to study the inverse source problem. In Sec. 3, the forward and inverse problems are solved using the circular harmonics expansion, and the proposed stable algorithm is presented. In Sec. 4 shows numerical examples of the proposed algorithm for the case where the source is a harmonic function. In Sec. 5 presents an inverse source problem in optics, considering that the source is harmonic. In Sec. 6 studies the same inverse source problem in optics considering a priori information about the source. Finally, the conclusions are given in Sec. 7.

2. Mathematical model

The problem that concerns us is related to the following boundary value problem.

$$\begin{aligned} \Delta u &= f \quad \text{in} \quad \Omega, \\ \frac{\partial u}{\partial n} &= 0 \quad \text{on} \quad \partial\Omega, \end{aligned} \tag{1}$$

where Ω is a bounded region sufficiently smooth, Δ represents the Laplace operator, f is called the *source* and u is the

potential defined in $\overline{\Omega}$. The boundary condition on $\partial\Omega$ can be interpreted as a null flux condition. The Laplace operator is also denoted by ∇^2.

There are two problems associated with problem (1), which are given in the following definitions: The first one is called the *forward problem*, which consists of determining the potential u (measurement) on the boundary when the source is known. The second one is called the *inverse problem*, which is defined as follows:

Given a measurement V, the inverse problem consists of determining a source such that the solution u of the boundary value problem (1) *satisfies that $u|_{\partial\Omega} = V$.*

From the Green formulas, we get the following compatibility condition.

$$\int_\Omega f d\Omega = 0. \tag{2}$$

2.1. Weak solution and operational statement

The following definitions can be found in Ref. [9].

Let $L_2(\Omega)$ and $L_2(\partial\Omega)$ be the spaces of square integrable functions defined on Ω and $\partial\Omega$, respectively, that take real values. $H^1(\Omega)$ is the Sobolev space consisting of functions in $L_2(\Omega)$ whose generalized first derivatives are also square integrable, where Ω is a bounded domain in $\mathbb{R}^n$, with boundary $\partial\Omega$ sufficiently smooth. $L_2(\Omega)$ is a normed vector space with the following norm

$$\|f\|_{L_2(\Omega)} = \left(\int_\Omega f^2 d\Omega\right)^{1/2}.$$

This norm arises from the scalar product

$$\langle f, g\rangle_{L_2(\Omega)} = \int_\Omega f g d\Omega.$$

Thus, $L_2(\Omega)$ is a Hilbert space. Analogously, we get that $L_2(\partial\Omega)$ is a Hilbert space.
$H^1(\Omega)$ is a normed vector space with the following norm

$$\|f\|_{H^1(\Omega)} = \|f\|_{L_2(\Omega)} + \|D^1 f\|_{L_2(\Omega)}, \tag{3}$$

where $D^1 f = (D_1^1 f, D_2^1 f)$ and D_i^1 is the operator of generalized first derivatives (see Appendix B). This norm arises from the scalar product

$$\langle f, g\rangle_{H^1(\Omega)} = \langle f, g\rangle_{L_2(\Omega)} + \langle D^1 f, D^1 g\rangle_{L_2(\Omega)},$$

from where $H^1(\Omega)$ is also a Hilbert space. The space $H^1(\Omega)$ also is the completeness of the $C^1(\overline{\Omega})$ when we consider the norm (3). This result can be found in [9], p.p. 59-60.
So, we consider the following spaces:

$$\mathcal{U} = \left\{ f \in L_2(\Omega) \,:\, \int_\Omega f \, d\Omega = 0 \right\},$$

$$\mathcal{V} = \left\{ u \in H^1(\Omega) \,:\, \int_\Omega u \, d\Omega = 0 \right\},$$

$$\mathcal{W} = \left\{ v \in L_2(\partial\Omega) \,:\, \int_{\partial\Omega} v \, d\partial\Omega = 0 \right\}.$$

The space $\mathcal{W}$ is called the spaces of measurement functions. In this space is the image of the operator A, which relates the sources f with the measurement V, i.e., given a source f, the solution of the forward problem gives an ideal measurement $A(f) = V \in \mathcal{W}$. This ideal measurement is defined on $\partial\Omega$, and the real measurement is recorded in a finite number of points on the same $\partial\Omega$, which can be interpolated to get an element of the $L_2(\mathcal{W})$, which must be close to the ideal measurement (i.e., an element of $\mathcal{W}$). Since the real measurement contains errors, we have to interpolate in a stable form. We can use different interpolation methods to get an element of $\mathcal{W}$. In this work, we consider that the measurement is expressed as Fourier series and that we know the Fourier coefficients.

Using the Green formulas, the following definition is obtained, which can be found in [10], p. 171.

Definition 1. *Given $f \in \mathcal{U}$, the function $u \in \mathcal{V}$ is called the weak solution of the problem (1) if it satisfies*

$$\int_\Omega \nabla u \cdot \nabla v d\Omega = \int_\Omega f v ds, \tag{4}$$

for all $v \in H^1(\Omega)$.

The following Theorem can be found in Ref. [10]:

Theorem 1. *Given $f \in \mathcal{U}$, the problem (1) has a unique solution $u \in \mathcal{V}$, which satisfies*

$$\|u\|_{H^1(\Omega)} \leq C(\Omega) \|f\|_{L_2(\Omega)}, \tag{5}$$

where the constant $C(\Omega)$ does not depend on f.

We can define the operator $T : \mathcal{U} \to \mathcal{V}$ such that $T(f) = u$ where $u \in \mathcal{V}$ is the solution of the problem (1). As well, we define the operator trace $tr : \mathcal{V} \to \mathcal{W}$ such that $tr(u) = V$ where $u \in \mathcal{V}$ is the weak solution of the problem (1), *i.e.*, the operator trace is the generalization of the restriction of the function u on $\partial\Omega$ (see Appendix B). The operator trace evaluated in u is also denoted by $u|_{\partial\Omega} = V$. The operator $A = tr \circ T$, which is composition of T with the trace $tr : \mathcal{V} \to \mathcal{W}$, is compact since tr is compact, which relates the source f with the measurement $V = u|_{\partial\Omega}$. In terms of the operator A, the inverse problem can be stated as follows:

Given a function $V \in \mathcal{W}$ find a source $f \in \mathcal{U}$ such that

$$A(f) = V. \tag{6}$$

The operator A is not injective, which is a consequence of the Theorem 2, which can be found in Ref. [11]. In this Theorem, it was proved that $\ker(A) \neq \{0\}$. Since A is linear, it is not injective.

Theorem 2. $\ker(A) = [Harm(\Omega)]^{\perp}$, *where* $Harm(\Omega)$ *represents the space of harmonic functions defined in* Ω.

We denote by $H^{\perp}(\Omega)$=$\{g \in Harm(\Omega) : \langle g, 1\rangle_{L_2(\Omega)} = 0\}$. We have $\mathcal{U} = \ker(A) \bigoplus H^{\perp}(\Omega)$. This Theorem shows that the space $\mathcal{U}$ can be decomposed in a direct sum of the space of harmonic functions and its orthogonal space, which is the kernel of the operator A. This decomposition is a consequence of the Theorem 1 given in Ref. [12] p. 53 since the space of harmonic functions is closed. From Theorem 2, the restriction $\hat{A}$ of the operator A to $H^{\perp}(\Omega)$ is injective, *i.e.,* we can recover uniquely the harmonic component f_h of the source from the measurement V. Since $\hat{A}$ is compact, the inverse $\hat{A}^{-1}$ is not continuous, which is related to the ill-posedness of the problem. More precisely, the no continuity of the operator $\hat{A}^{-1}$ is associated with the numerical instability (see Appendix D).

To recover the whole source $f \in \mathcal{U}$, we have to impose a priori information to find its non-harmonic component. In Ref. [4], the source is given by a product of two functions that depend on different variables, one of them is known considering a cylindrical geometry. In Ref. [5], the authors recover the non-harmonic component of the source using a priori information and an iterative algorithm for some particular classes of sources. For example, the authors consider the case when the whole source is harmonic in a subdomain of the region. Synthetic examples are developed in circular (simple) and irregular (complex) regions to validate the numerical methodology.

For simplicity of the notation, in what follows, we will use the symbol A to denote the operator $\hat{A}$.

2.2. Tikhonov regularization

In practice, we know V_δ instead V with $\|V - V_\delta\|_{L_2(\partial\Omega)} < \delta$ where $\delta > 0$ is called the measurement error. To handle the numerical instability of the operational equation $A(f) = V$, the Tikhonov regularization method is used, which consists of adding a regularization (penalization) term to the least square problem $J(f) = \frac{1}{2}\|A(f) - V\|^2_{L_2(\partial\Omega)}$, that is, the method minimizes the regularized functional

$$J_\alpha(f) = \frac{1}{2}\|A(f) - V\|^2_{L_2(\partial\Omega)} + \frac{\alpha}{2}\|f\|^2_{L_2(\Omega)}, \qquad (7)$$

where $\alpha(\delta) > 0$ is the Tikhonov regularization parameter, which must be chosen appropriately in terms of the error δ [1, 13].

Let $f_{\alpha(\delta)} = R_\alpha V_\delta$ be an approximation of f_h where $R_\alpha = (A^*A + \alpha I)^{-1}A^*$ is the operator associated with the Tikhonov regularization strategy, which has the properties described in the following theorems ([1, 13]):

Theorem 3. $R_\alpha : H^{\perp}(\Omega) \to L_2(\partial\Omega)$ *is boundedly invertible, and* $f_{\alpha(\delta)} = R_\alpha V_\delta$ *is the unique solution of the normal equation* $(A^*A + \alpha I)f_{\alpha(\delta)} = A^*V_\delta$. *Furthermore,* $\|R_\alpha\| \leq 1/\sqrt{\alpha}$.

Theorem 4. *Any choice* $\alpha(\delta)$ *such that* $\lim_{\delta\to 0}\alpha(\delta) = 0$ *and* $\lim_{\delta\to 0}\delta^2 / \alpha(\delta) = 0$ *ensures that*

$$\sup\big\{\|R_\alpha V_\delta - A^{-1}V\|_{L_2(\Omega)} : V_\delta \in L_2(\partial\Omega), \\ \|V - V_\delta\|_{L_2(\partial\Omega)} \leq \delta\big\} \to 0,$$

when $\delta \to 0$. In this case, R_α is called '*admissible*' and

$$\lim_{\delta\to 0} f_{\alpha(\delta)} = f_h \quad \text{in} \quad L_2(\Omega). \qquad (8)$$

There are different methods for determining a suitable regularization parameter that should balance the two terms of the functional J_α. The discrepancy principle and the L-curve are examples of these methods. The name L-curve comes from the shape of the curve and is a log-log plot of the norm of a regularized solution versus the norm of the corresponding residual norm [14].

In this work, we consider two regularization parameters: The first one is the Tikhonov parameter, and the second one is the term where the expansion series is truncated.

We will denote the operator $\hat{A}$ by A.

3. Solving the forward and inverse problems

3.1. Circular regions

We consider that the region Ω is a circular region of radius R centered in the origin. The source can be expressed by

$$f(r,\theta) = \sum_{k=1}^{\infty} f_k^1 A_k r^k \cos k\theta + f_k^2 A_k r^k \sin k\theta, \qquad (9)$$

where $A_k = \sqrt{2k+2}/(R^{k+1}\sqrt{\pi})$ is a normalization factor, and $f_k^1 = \langle f, A_k r^k \cos k\theta\rangle_{L_2(\Omega)}$, $f_k^2 = \langle f, A_k r^k \sin k\theta\rangle_{L_2(\Omega)}$ are the Fourier coefficients, $k = 1, 2 \ldots$.

The solution of the problem (1) is sought in the form

$$u(r,\theta) = \sum_{k=1}^{\infty} a_k A_k r^k \cos k\theta + b_k A_k r^k \sin k\theta \\ + \sum_{k=1}^{\infty} c_k B_k r^{k+2} \cos k\theta + d_k B_k r^{k+2} \sin k\theta, \qquad (10)$$

where $B_k = \sqrt{2k+6}/(R^{k+3}\sqrt{\pi})$ is a normalization factor.

After some calculations, we found (see Appendix A):

$$a_k = \Gamma_k f_k^1, \quad b_k = \Gamma_k f_k^2, \\ c_k = \Lambda_k f_k^1, \quad d_k = \Lambda_k f_k^2. \qquad (11)$$

where $\Gamma_k = -(k+2)R^2/(4k(k+1))$ and $\Lambda_k = R\sqrt{k+1}/(4(k+1)\sqrt{k+2})$.

The solution of the forward problem is given by (see Appendix A):

$$A(f)(\theta) = V(\theta) = \sum_{k=1}^{\infty} C_k \frac{\cos k\theta}{\sqrt{\pi}} + D_k \frac{\sin k\theta}{\sqrt{\pi}}, \quad (12)$$

where $C_k = \sqrt{\pi}\left(a_k A_k R^k + c_k B_k R^{k+2}\right)$ and $D_k = \sqrt{\pi}\left(b_k A_k R^k + d_k B_k R^{k+2}\right)$.

For the inverse problem, we consider that the exact measurement is given by

$$V(\theta) = \sum_{k=1}^{\infty} V_k^1 \frac{\cos k\theta}{\sqrt{\pi}} + V_k^2 \frac{\sin k\theta}{\sqrt{\pi}}, \quad (13)$$

where the Fourier coefficients V_k^1 and V_k^2 of V are known.

To find the minimum of $J_{\alpha(\delta)}$ we have to solve the normal equations:

$$\left[A^* A + \alpha(\delta) I\right](f) = A^* V,$$

where $A^* : \mathcal{W} \to \mathcal{U}$ is the adjoint operator of A, which is given by $A^*(\psi) = -\varphi$ where φ is the solution of the adjoint boundary value problem [5, 11]

$$\begin{aligned} &\Delta\varphi = 0 \quad \text{in} \quad \Omega, \\ &\frac{\partial\varphi}{\partial n} = \psi \quad \text{on} \quad \partial\Omega. \end{aligned} \quad (14)$$

When Ω is a circle of radius R centered in the origin, the operator A^* is given by (see Appendix A) [6]:

$$A^*(\psi)(r,\theta) = -\sum_{k=1}^{\infty} E_k \times \left[\psi_k^1 A_k r^k \cos k\theta + \psi_k^2 A_k r^k \sin k\theta\right], \quad (15)$$

where

$$\psi(\theta) = \sum_{k=1}^{\infty} \psi_k^1 \frac{\cos k\theta}{\sqrt{\pi}} + \psi_k^2 \frac{\sin k\theta}{\sqrt{\pi}}$$

and

$$E_k = \frac{R}{\sqrt{\pi} k A_k R^k}.$$

Instead of V, we consider the measurement with error

$$V_\delta(\theta) = \sum_{k=1}^{\infty} V_{k,\delta}^1 \frac{\cos k\theta}{\sqrt{\pi}} + V_{k,\delta}^2 \frac{\sin k\theta}{\sqrt{\pi}}, \quad (16)$$

with $\|V - V_\delta\|_{L_2(\partial\Omega)} \leq \delta$. After substituting in the normal equations, we get the regularized solution:

$$f_{\alpha(\delta)} = \sum_{k=1}^{\infty} \overline{A}_k A_k \left[V_{k,\delta}^1 r^k \cos k\theta + V_{k,\delta}^2 r^k \sin k\theta\right], \quad (17)$$

where

$$\overline{A}_k = \frac{E_k}{\sqrt{\pi} E_k \Phi_k - \alpha}, \quad (18)$$

and $\Phi_k = \Gamma_k A_k R^k + \Lambda_k B_k R^{k+2}$.

4. Algorithm to recover the harmonic function

From (17), we obtain the following stable algorithm to recover the source from the measurement with errors V_δ:

Algorithm 1: To identify the harmonic source we proceed as follows:

Step 1. We take some values for the parameters σ_1, σ_2, R_1, R_2 and we take a source g defined on Ω.

Step 2. We solve the boundary value problem (1).

Step 3. We compute the $V = u|_{\partial\Omega}$, the exact measurement, using Eq. (12) for $N = 30$, which was chosen by numerical tests.

Step 4. To emulate the measurement with error, we aggregate an appropriate random error, using the *rand* function of MATLAB, to the coefficients V_k^1 and V_k^2, where $k = 1, 2....$ Hence, we get the coefficients $V_{k,\delta}^1$ and $V_{k,\delta}^2$, $k = 1, 2...$ of the measurement with error V_δ, which satisfies $\|V_\delta - V\|_{L_2(\partial\Omega)} \leq \delta$.

Step 5. Then, we get the regularized solution to the inverse problem by

$$f_{\alpha(\delta)}^N = \sum_{k=1}^{N} \overline{A}_k A_k \left[V_{k,\delta}^1 r^k \cos k\theta + V_{k,\delta}^2 r^k \sin k\theta\right], \quad (19)$$

taking $\alpha(\delta) = 10^{-5}$ and $N = 16$.

According to the numerical results obtained in this work, we propose the following values for the regularization parameters: $\alpha = 10^{-5}$ and $N = 16$, which is an original result.

Considering a prior information, we can get estimates about the convergence of the regularized solution (see Appendix C). A prior information is obtained from the specialist on the topic studied.

5. Numerical example

In this section, we illustrate the algorithm proposed by synthetic examples proceeding as in the following:

Example 1. We consider the source $f(x,y) = e^x \cos y$, defined in the circular region $\Omega = \left\{(x,y) : x^2 + y^2 < 1\right\}$. In polar coordinates, $f(r,\theta) = e^{r\cos\theta}\cos(r\sin\theta)$. In Figs. 1 and 2 show the exact source and its approximations by Fourier series using $N = 16$ terms in (9). The error between the approximated and exact source is 0.0872. In Fig. 3 shows the potential obtained using (10) and the measurement with and without error. In Fig. 5 shows the recovered source using the Algorithm 1, which take $N = 16$ and $\alpha = 10^{-5}$. In Figs. 6 and 7 show the importance of the two regularization parameters. In Fig. 6, we take $\alpha = 10^{-5}$ and $N = 100$.

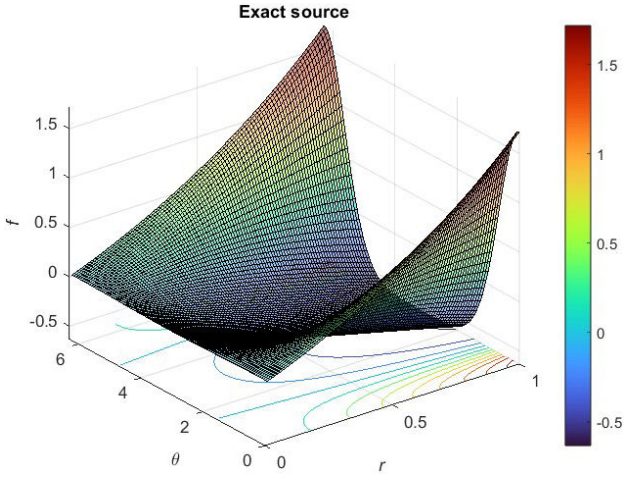

FIGURE 1. Exact source.

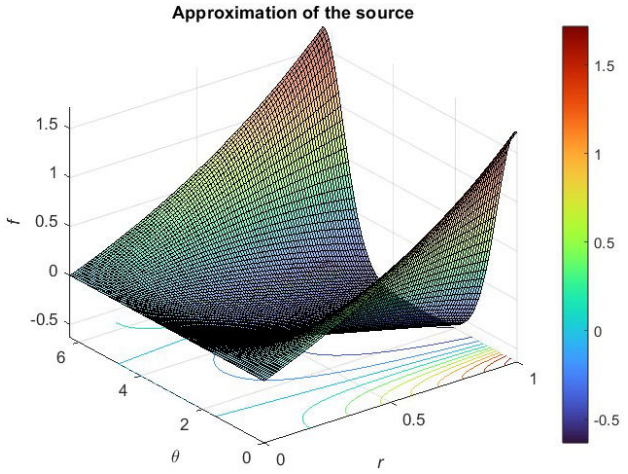

FIGURE 2. Approximated source obtained taking $N = 16$ terms in (9).

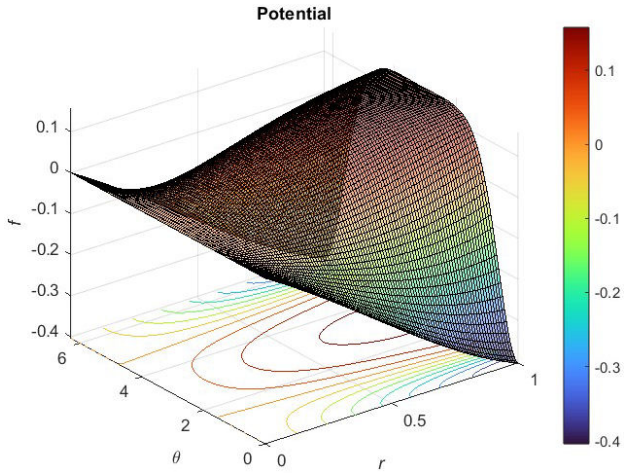

FIGURE 3. Potential obtained using (10) taking $N = 16$ terms.

In Fig. 7, we take $\alpha = 0$ and $N = 16$. Similar results are obtained for other values of the two regularization parameters α and N. Table I shows the regularized solution for different parameter values α and for different values of the error δ.

TABLE I. Relative errors for different values of δ and Tikhonov regularization parameter taking $N = 16$ for the truncation of the series.

α	$\delta = 0.1$	$\delta = 0.05$	$\delta = 0.01$	$\delta = 0.001$
10^{-3}	0.1128	0.6765	0.0103	0.0076
10^{-4}	0.1332	0.0467	0.0112	0.0041
10^{-5}	0.0890	0.0580	0.0142	0.0031
10^{-6}	0.0879	0.0645	0.0100	0.0030
10^{-7}	0.1089	0.0535	0.0138	0.0039

TABLE II. Absolute errors for different values of the Tikhonov regularization parameter α and different values of the truncation parameter N, with $\delta = 0.1$.

α	$N = 16$	$N = 30$	$N = 60$	$N = 100$
10^{-3}	0.3810	0.5375	0.5813	0.7628
10^{-4}	0.3064	0.4095	0.8857	0.9052
10^{-5}	0.2879	0.5586	0.7544	1.0085
10^{-6}	0.3350	0.4025	1.0836	1.1301
10^{-7}	0.3106	0.6872	0.5617	0.8671

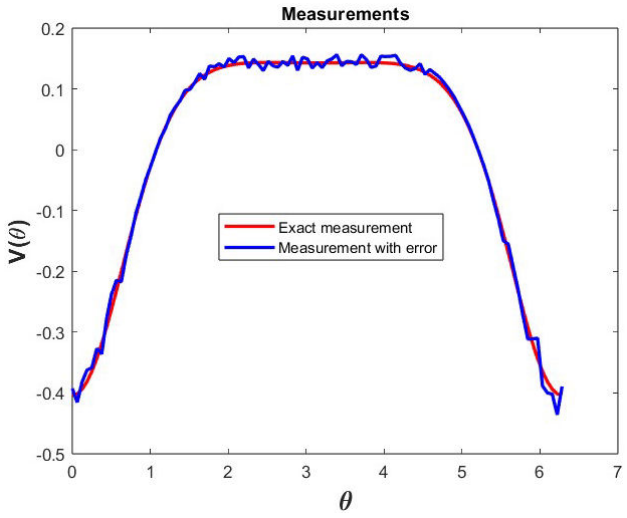

FIGURE 4. Measurements without and with error in red and blue, respectively.

We can observe that the parameters $\alpha = 10^{-6}$ and $N = 16$ give good results. Table II shows the numerical results for other values of N and α. The optimal values are $N = 16$ and $\alpha = 10^{-5}$, for $\delta = 0.1$.

6. Application to one optical problem

It has been shown in previous works that if a wavefront, which propagates in the direction of the optical axis, is considered within the paraxial approximation, we obtain the irradiance transport equation (ITE) [15]:

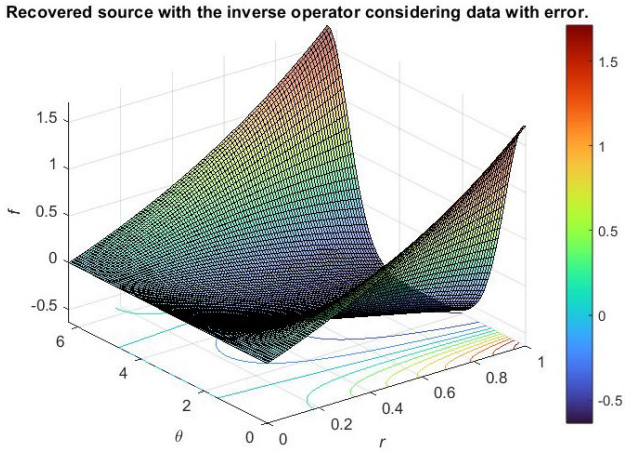

FIGURE 5. Recovered source taking $\delta = 0.1$, $\alpha = 10^{-5}$ and $N = 16$.

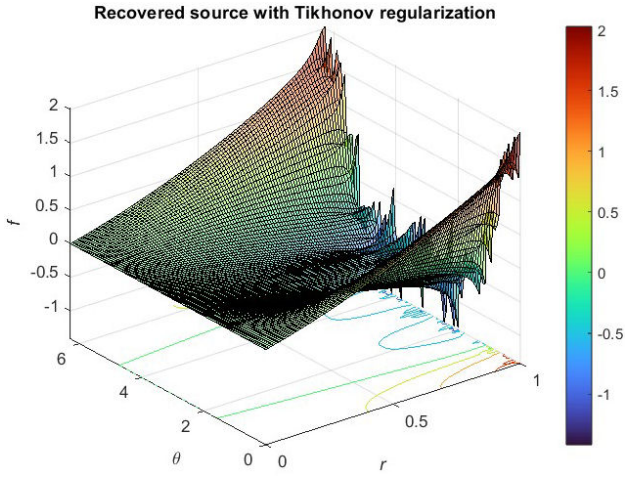

FIGURE 6. Recovered source taking $\delta = 0.1$, $\alpha = 10^{-5}$ and $N = 100$.

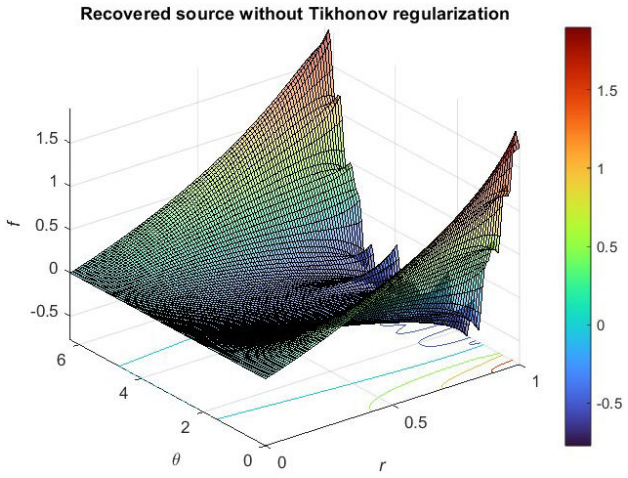

FIGURE 7. Recovered source taking: $\alpha = 0$, $\delta = 0.1$ and $N = 16$.

$$\nabla_T I \cdot \nabla_T W + I\nabla_T^2 W = -\frac{\partial I}{\partial z}. \tag{20}$$

The Eq. (20) is only valid in cases where the curvature presented during the wavefront propagation is smooth and the propagation of the wavefront is mainly in the paraxial regime [15].

The ITE is used in many schemes for recovering the phase from irradiance measurements, without using interferometric techniques. In addition, this transport equation is the basis for curvature wavefront sensing methods [16]. The ITE relates the phase in a plane orthogonal to the optical axis to the rate of change of the beam intensity along the propagation direction, assuming a paraxial beam described by $\Psi(x,y,z) = [I(x,y,z)]^{1/2}\exp[i\phi(x,y,z)]$, where $I(x,y,z)$ is the irradiance, and $\phi(x,y,z)$ is the phase. In terms of the wavefront $W(x,y,z)$, the phase is given by the relation $\phi(x,y,z) = (2\pi/\lambda)W(x,y,z) = kW(x,y,z)$ [16].

If the intensity distribution is considered to be almost uniform, the first term of Eq. (20) vanishes and the ITE becomes a Poisson equation as follows [8, 16, 17]:

$$\nabla_T^2 W = f, \tag{21}$$

where

$$f = -\frac{1}{I}\frac{\partial I}{\partial z}. \tag{22}$$

We can consider that

$$\frac{\partial W}{\partial n} = 0, \tag{23}$$

since that boundary condition is obtained by forcing the radial derivative to zero within a narrow band surrounding the boundaries [18].

Inverse problem: Given a measurement ϕ on the boundary $\partial\Omega$, to determine the source f such that the solution of (21)-(23) satisfies $W|_{\partial\Omega} = \phi$.

When we find f in a stable form applying our method, the irradiance I is given by:

$$I(z) = e^{-f(x,y)z}. \tag{24}$$

We consider the same procedure given in Section Numerical Example to solve the inverse problem when the measurement with error V_δ is known.

Example 2. *We consider in* (22) *the source given by* $f(x,y) = x^2 - y^2$ *defined in the circular region* $\Omega = \{(x,y) : x^2 + y^2 < 1\}$. *In polar coordinates,* $f(r,\theta) = r^2\cos(2\theta) = f_2^1 A_2 r^2\cos(2\theta)$ *where* $f_2^1 = 1/A_2$ *is the unique Fourier coefficient different to zero. The solution of the problem* (21)-(23) *is*

$$u(r,\theta) = \frac{r^4 - 2r^2}{12}\cos 2\theta, \tag{25}$$

which in x-y *coordinates is given by*

$$u(x,y) = \frac{(x^2+y^2-2)(x^2-y^2)}{12}.$$

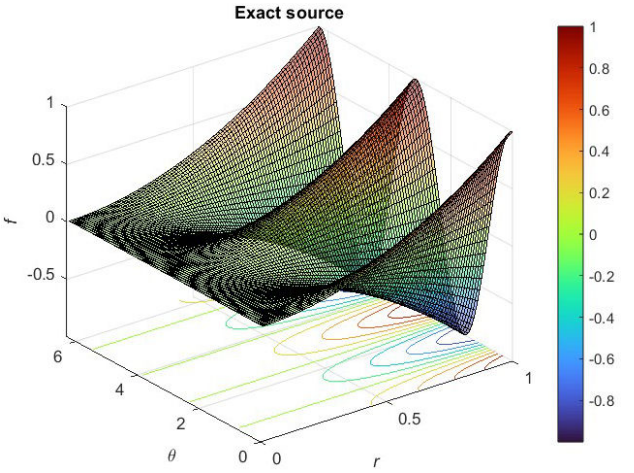

FIGURE 8. Exact source.

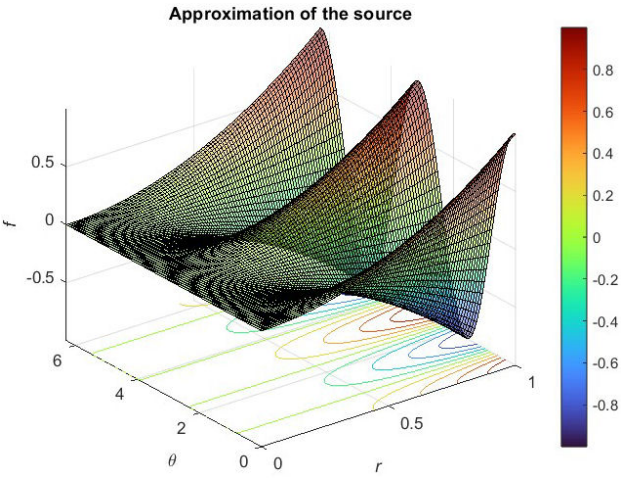

FIGURE 9. Approximated source obtained taking $N = 16$ terms in (9).

In this case, the measurement V is given by

$$V(\theta) = V_2^1 \frac{\cos 2\theta}{\sqrt{\pi}}, \tag{26}$$

where $V_2^1 = (R^4 - 2R^2/12)\sqrt{\pi}$ is the unique Fourier coefficient different to zero.

In Fig. 8 and 9 show the exact source and its approximation using the Fourier series taking $N = 16$ terms of the expansion. In Fig. 10 shows the solution to the problem. In Fig. 11 shows the exact and with error measurements, denoted by V and V_δ, respectively. In Fig. 12 and 14 respectively show the recovered sources with and without regularization. Table III shows the relative errors for different error values δ and different values of the Tikhonov regularization parameter. We consider $N = 16$ for the truncation of the series (9). The numerical results show the feasibility of the proposed method.

Example 3. *We consider in* (22) *the source given by* $f(x, y) = x^3 - 3xy^2$ defined in the circular region $\Omega = \{(x, y) : x^2 + y^2 < 1\}$. *In polar coordinates,* $f(r, \theta) = r^3 \cos^3(\theta) - 3r\cos(\theta)r^2 \sin^2(\theta)$.

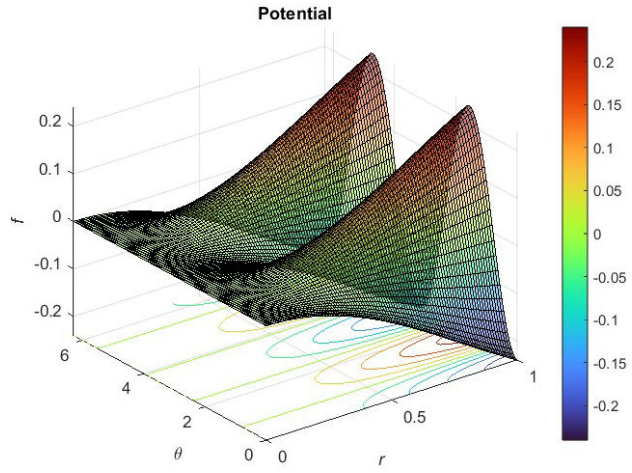

FIGURE 10. Potential obtained using (10) taking $N = 16$ terms.

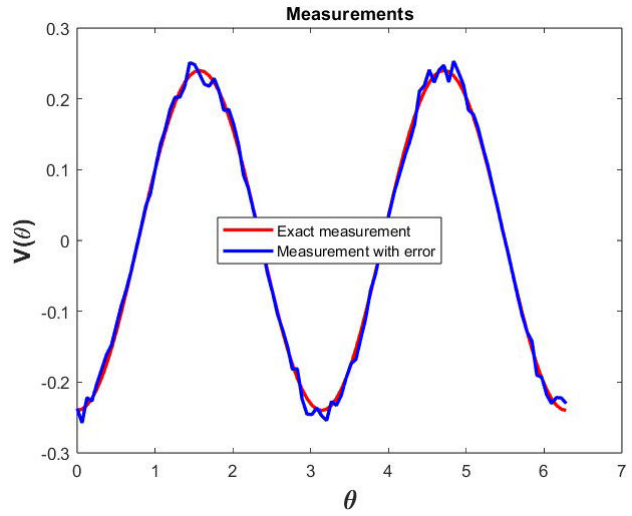

FIGURE 11. Measurements without and with error in red and blue, respectively.

TABLE III. Relative errors for different values of δ and Tikhonov regularization parameter taking $N = 16$ for the truncation of the series.

α	$\delta = 0.1$	$\delta = 0.05$	$\delta = 0.01$	$\delta = 0.001$
10^{-3}	0.1180	0.0859	0.0164	0.0168
10^{-4}	0.1450	0.0821	0.0158	0.0089
10^{-5}	0.1705	0.0605	0.0175	0.0074
10^{-6}	0.1785	0.0576	0.0152	0.0078
10^{-7}	0.1476	0.0820	0.0150	0.0089

In Fig. 15 and 16 show the exact source and its approximation using the Fourier series taking $N = 16$ terms of the expansion. In Fig. 18 shows the exact and with error measurements, denoted by V and V_δ, respectively. In Fig. 19 and 21 show the recovered sources with and without regularization.

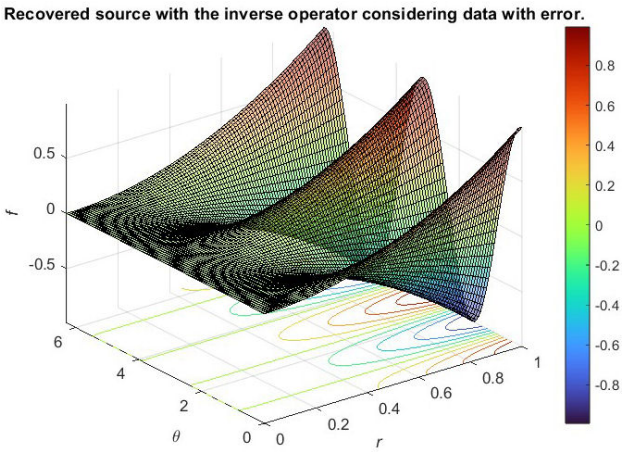

FIGURE 12. Recovered source taking $\delta = 0.1$, $\alpha = 10^{-5}$ and $N = 16$.

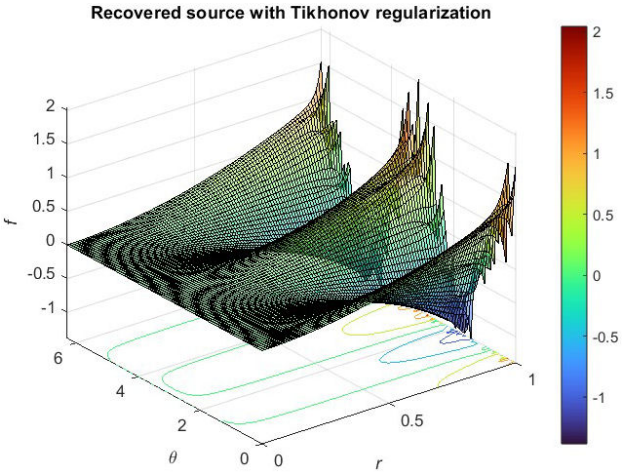

FIGURE 13. Recovered source taking $\delta = 0.1$, $\alpha = 10^{-5}$ and $N = 100$.

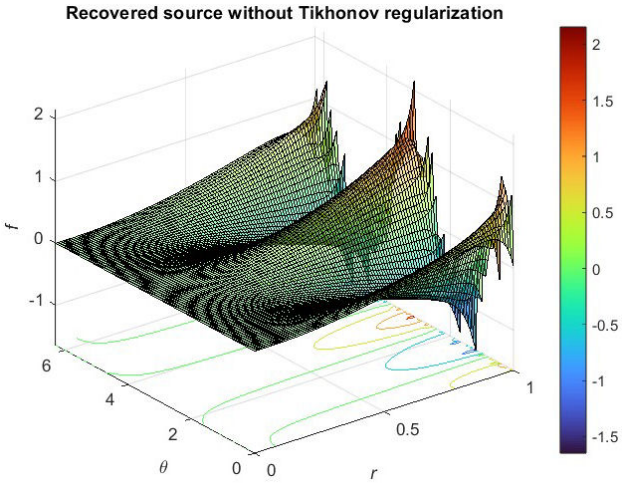

FIGURE 14. Recovered source taking: $\alpha = 0$, $\delta = 0.1$ and $N = 16$.

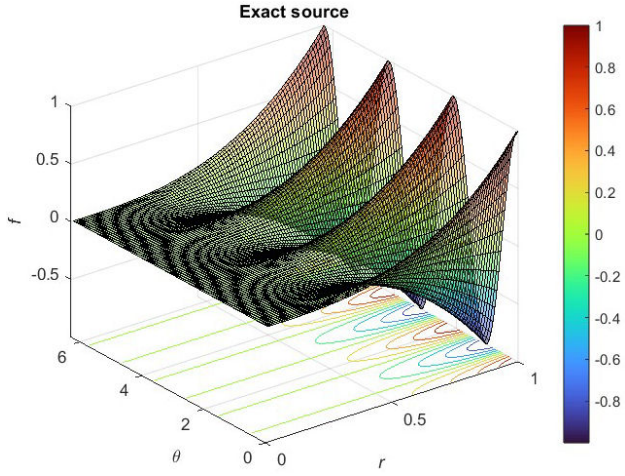

FIGURE 15. Exact source.

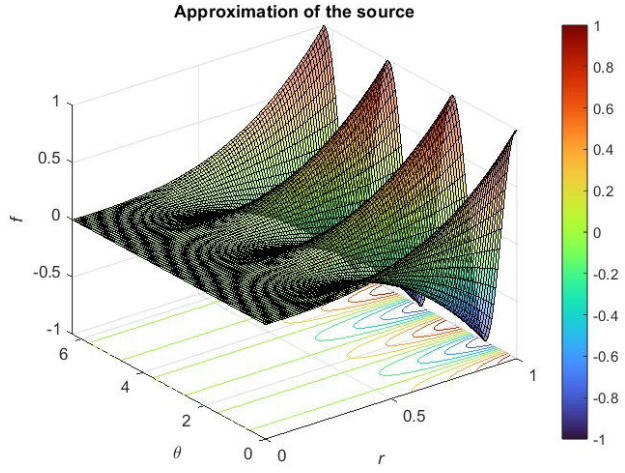

FIGURE 16. Approximated source obtained taking $N = 16$ terms in (9).

TABLE IV. Relative errors for different values of δ and Tikhonov regularization parameter taking $N = 16$ for the truncation of the series.

α	$\delta = 0.1$	$\delta = 0.05$	$\delta = 0.01$	$\delta = 0.001$
10^{-3}	0.1444	0.0902	0.0197	0.0181
10^{-4}	0.1714	0.1034	0.0191	0.0083
10^{-5}	0.2039	0.0681	0.0151	0.0071
10^{-6}	0.2116	0.0669	0.0199	0.0065
10^{-7}	0.1710	0.0929	0.0179	0.0077

7. Information a priori: the sources are defined in a circle contained in the region

We consider a special case regarding the problem of recovering the whole source, which will be described below in detail.

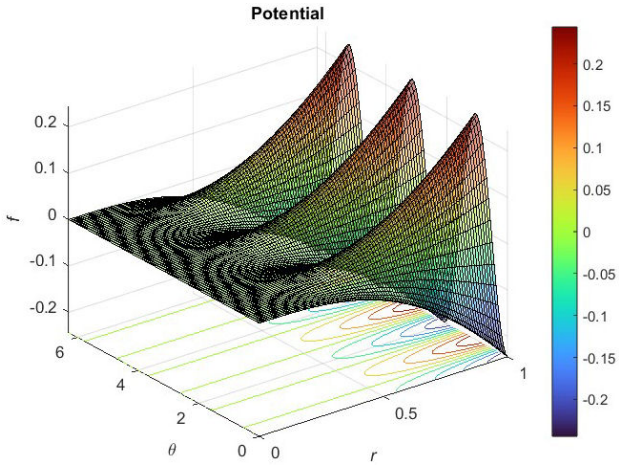

FIGURE 17. Potential obtained using (10) taking $N = 16$ terms.

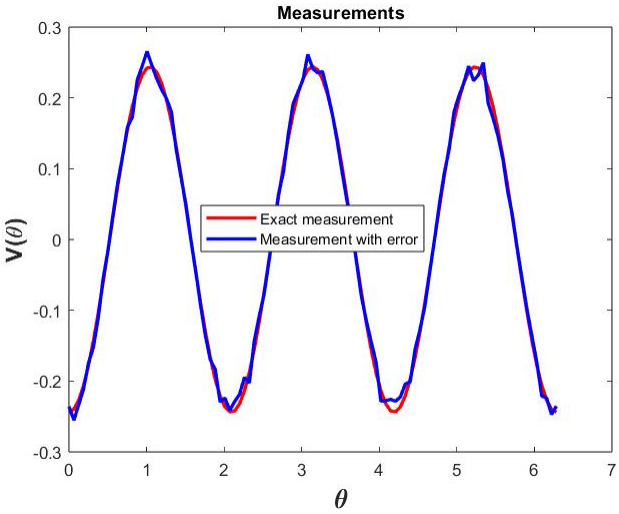

FIGURE 18. Measurements without and with error in red and blue, respectively.

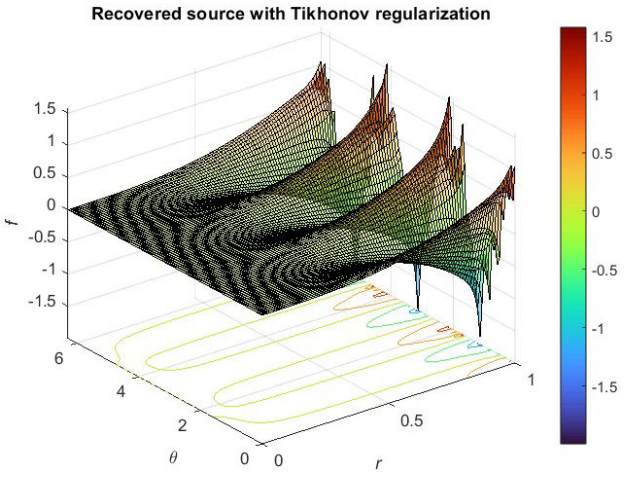

FIGURE 19. Recovered source taking $\delta = 0.1$, $\alpha = 10^{-5}$ and $N = 100$.

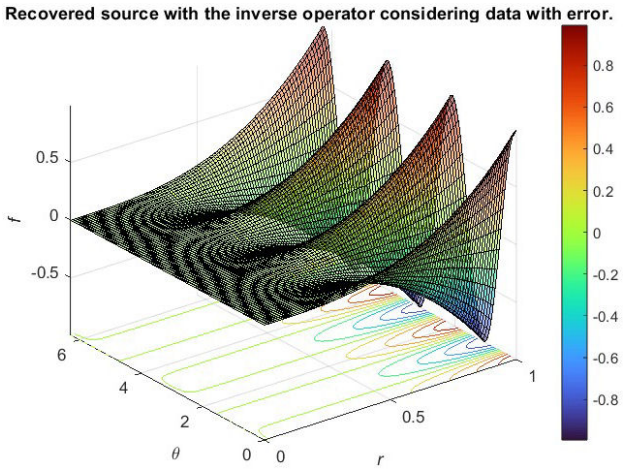

FIGURE 20. Recovered source taking $\delta = 0.1$, $\alpha = 10^{-5}$ and $N = 16$.

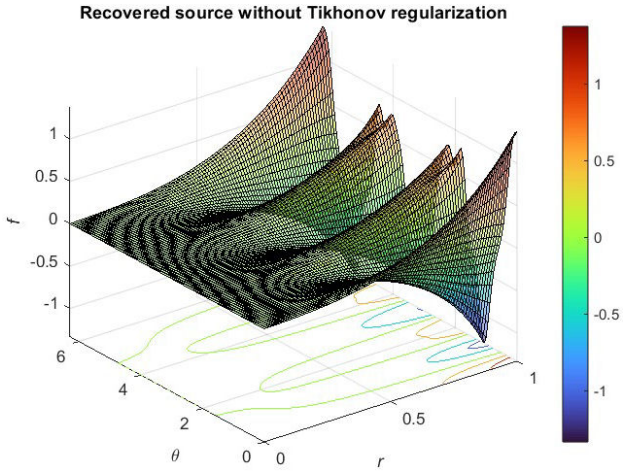

FIGURE 21. Recovered source taking: $\alpha = 0$, $\delta = 0.1$ and $N = 16$.

7.1. Identification of Non-Harmonic sources

According to Theorem 2, we know that a general source $f \in \mathcal{U}$ is the direct sum of two sources; one of them is a harmonic function, and the other one belongs to $\ker(A)$, *i.e.*,

$$f = f_0 + h, \quad \text{with} \quad f_0 \in \ker(A), \quad \text{and } h \in H^{\perp}(\Omega). \tag{27}$$

In previous sections, we have dealt with the computation of the harmonic part h, which can be recovered from measurements on the exterior boundary $\partial\Omega$. We emphasize that *f and h produce the same measurement since f_0 produces the measurement zero.*

7.2. Describing the class of functions

In this section, we are concerned with the non-harmonic component f_0, which can be identified using a priori information.

Let $\mathcal{F}$ be a class of piecewise sources that take two constant values α and β known in Ω, such that f takes the value α in a subset $U \subset \overline{\Omega}$ and β in $(\overline{\Omega} \cap (U^c))$. We consider the subclass $\mathcal{F}_c$ of sources $f_{\mathbf{x}_0}$ such that the sets $U = \{\mathbf{x} \in \overline{\Omega} : f_{\mathbf{x}_0}(\mathbf{x}) = \alpha\}$ are closed circles contained in $\overline{\Omega}$ with $\mu(U) > 0$, where all circles U have the same radius. Let $\mathbf{x}_0 \in \Omega$ be the center and $R_0 > 0$ the radius of U. Then, each $f_{\mathbf{x}_0} \in \mathcal{F}_c$ is of the form

$$f_{\mathbf{x}_0} = (\alpha - \beta)\,\chi_U + \beta, \tag{28}$$

where χ_U is the indicator function of U. Since f_{x_0} must be orthogonal to the constants, we obtain

$$\begin{aligned} 0 &= \int_{\Omega_1} f_{\mathbf{x}_0}\, d\mathbf{x} = (\alpha - \beta)\,\mu(U) + \beta\,\mu(\Omega) \\ &= \alpha\,\mu(U) + \beta\,\mu(\Omega \setminus U), \end{aligned} \tag{29}$$

where μ denotes the Lebesgue measure on the plane. So the parameter β is given by

$$\beta = \frac{-\alpha\mu(U)}{\mu(\Omega \setminus U)} = \frac{-\alpha\mu(U)}{\mu(\Omega) - \mu(U)}, \tag{30}$$

and taking into account (29)

$$\mu(U) = \frac{\beta}{\beta - \alpha}\mu(\Omega) = \frac{\beta\pi R^2}{\beta - \alpha}. \tag{31}$$

If the sets U are circles contained in $\overline{\Omega}$, then from (31) all these circles must have the same radius:

$$R_0 = \sqrt{\frac{\beta}{\beta - \alpha}}R. \tag{32}$$

The center $x_0 = (x_0^1, x_0^2)$ of these circles U must be contained in the disk centered at $(0,0)$ and radius $R - R_0 = \left(1 - \sqrt{\beta/(\beta - \alpha)}\right) R$. From (29), it is concluded that α and β must have opposite signs. Furthermore, all $f_{\mathbf{x}_0} \in \mathcal{F}_c$ can also be written as

$$f_{\mathbf{x}_0} = (\alpha - \beta)\,\left[\chi_U - \frac{\mu(U)}{\mu(\Omega)}\right]. \tag{33}$$

for some convex closed set U in $\overline{\Omega}$ and satisfies (29).

7.3. Uniqueness of the identification problem in a class of piecewise constant sources

The following Theorems can be found in Ref. [7].

Theorem 5. *For any family of convex closed subsets of $\overline{\Omega}$ satisfying condition (29), the corresponding family of functions $\mathcal{F}$ defined by (33) is a class of unicity for solving the inverse problem of identifying f in the EBP from the measurement ϕ.*

Theorem 6. *Any set $\mathcal{F}$ of functions orthogonal to the constants in Ω takes the value α on a convex closed set $\overline{\Omega}$, and β on its complement consists of functions of the form (33) with U closed convex contained in $\overline{\Omega}$ satisfying the restriction (29) with α and β fixed such that $\alpha\beta < 0$. Moreover, whatever the family $\mathcal{U}$ of closed convex sets with the properties mentioned, the corresponding set $\mathcal{F}$ is compact in $L_2(\Omega)$ and is contained in the sphere centered at O and radius $\sqrt{-\alpha\beta}R$, where R is the radius of the circular region Ω with center in the origin O.*

From the Theorem 5, the set $\mathcal{F}_c$ is a class of uniqueness used to identify the source $f_{\mathbf{x}_0}$ of the boundary problem (1) from a measurement V on $\partial\Omega$. To solve the inverse problem in a circular region Ω with conductivity σ, we applied Algorithm 2 of the Subsec, 7.4, when we have data with error in the measurement V_δ.

7.4. Stable algorithm for identification of piecewise constant sources

Algorithm 2: To identify a source $f_{\mathbf{x}_0} \in \mathcal{F}_c$, in the case when the measurement V_δ has error and $\|V_\delta - V\|_{L_2(\partial\Omega)} \leq \delta$.

Step 1. Find an approximated harmonic component of h from measurements with error V_δ on $\partial\Omega$ of $f_{\mathbf{x}_0}$ by Algorithm 1(given and illustrated in Sec. **??**). This approximated harmonic component is denoted by $h_{\alpha(\delta)}$.

Step 2. Determine the point $\mathbf{x}_\delta^0$ where $h_{\alpha(\delta)}(r,\theta)$ reaches its maximum value on $\partial\Omega$ (appealing to the maximum principle for harmonic functions in the bounded region $\overline{\Omega}$). The MATLAB *fmincon* routine may be employed to compute the point $\mathbf{x}_\delta^0$ where $h_{\alpha(\delta)}(r,\theta)|_{r=R}$ takes its maximum on $\partial\Omega$, which matches the minimum $-h_{\alpha(\delta)}(r,\theta)|_{r=R}$.

Step 3. Compute the unique center $\mathbf{x}_\delta^*$ of U by minimizing the following convex functional:

$$J_\delta(\mathbf{x}) = \| A(f_{\mathbf{x}}) - V_\delta \|^2_{L_2(\partial\Omega)}, \text{ for all } \mathbf{x} \in \Omega, \tag{34}$$

where A is the operator defined in (6). Of course, $f_{\mathbf{x}_0} \in \mathcal{F}_c$ also depends on the known radius R_0 of $\overline{U}$ (a priori information). This computed point $\mathbf{x}_\delta^*$ approximates $\mathbf{x}_0$. In this step, the MATLAB *fmincon* routine may be employed again to find the minimum point of the functional $J_\delta(\mathbf{x})$ expressed in polar coordinates:

$$\begin{aligned} J_\delta(r,\theta) = &\sum_{k=1}^{N(\delta)} \left(V^1_{k,\mathbf{x}} - V^1_{\delta,k}\right)^2 \\ &+ \left(V^2_{k,\mathbf{x}} - V^2_{\delta,k}\right)^2, \end{aligned} \tag{35}$$

where $V^i_{k,\mathbf{x}}$, $i = 1, 2$, are the coefficients with error of V_δ and the coefficients $V^i_{k,\mathbf{x}}$ depend on the variables r and θ. These are given by

$$V^1_{k,\mathbf{x}} = \frac{R^{k+2}h^1_{k,f_{\mathbf{x}}}}{2\sigma k(k+1)}, \quad \text{and} \quad V^2_{k,\mathbf{x}} = \frac{R^{k+2}h^2_{k,f_{\mathbf{x}}}}{2\sigma k(k+1)},$$

which are in terms of the Fourier coefficients $h^i_{k,f_{\mathbf{x}}}$, $i = 1, 2$, of the harmonic part h of the function $f_{\mathbf{x}}$. Taking into account (32) we have

$$h^1_{k,f_{\mathbf{x}}} = \langle f_{\mathbf{x}}, \rho^k \cos k\omega \rangle_{L_2(\Omega_1)} = (\alpha - \beta) \times \int_U \rho^k \cos k\omega d\Omega = (\alpha - \beta)\left(\pi R_0^2 r^k \cos k\theta\right) = -\beta R^2 r^k \cos k\theta, \quad (36)$$

and

$$h^2_{k,f_{\mathbf{x}}} = \langle f_{\mathbf{x}}, \rho^k \operatorname{sen} k\omega \rangle_{L_2(\Omega_1)} = (\alpha - \beta) \times \int_U \rho^k \operatorname{sen} k\omega d\Omega = (\alpha - \beta)\left(\pi R_0^2 r^k \operatorname{sen} k\theta\right) = -\beta R^2 r^k \operatorname{sen} k\theta, \quad (37)$$

where the center of the circles U in coordinates polar is $(r, \theta) \in [0, R - R_0] \times [0, 2\pi]$ and all them have the same radius R_0.

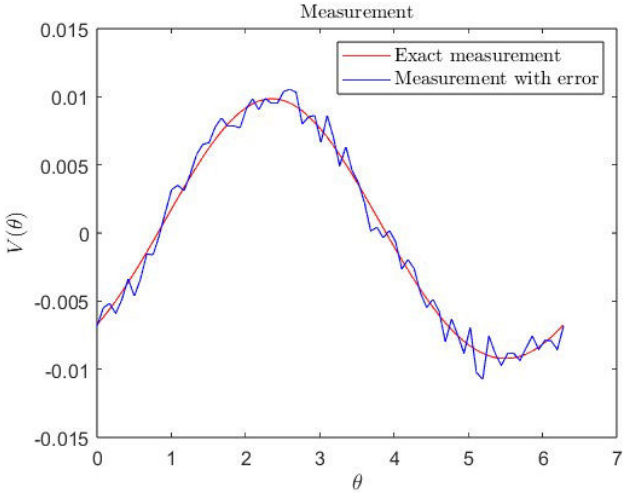

FIGURE 22. Plots of V (red) and V_δ (blue), for $\mathbf{x}_0 = (r_0, \theta_0) = (0.1, (3/4)\pi)$, $R_0 = 0.1$, $\alpha = 12$ and $\delta = 0.1$.

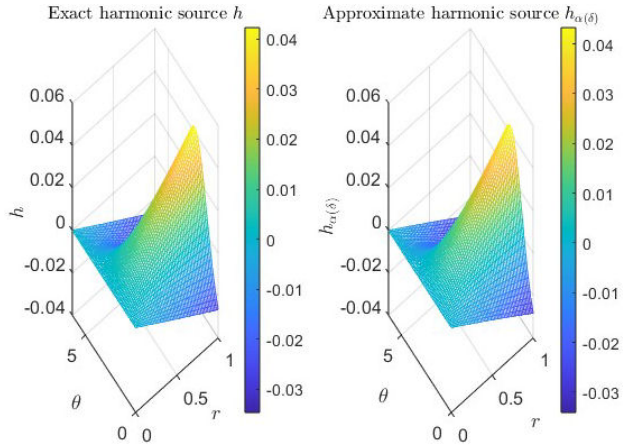

FIGURE 23. Recovered harmonic component $h_{\alpha(\delta)}$ (in region Ω) corresponding to the exact complete source $f_{\mathbf{x}_0} \in \mathcal{F}_c$, obtained with Algorithm 2 given in Subsec. 7.4, for $\mathbf{x}_0 = (r_0, \theta_0) = (0.1, (3/4)\pi)$, $R_0 = 0.1$, $\alpha = 12$ and $\delta = 0.1$.

Algorithm 2 is implemented *fmincon* routine to find the maximum of the approximated harmonic component on $\partial\Omega$, with a tolerance of 10^{-14}.

7.5. Numerical examples for piecewise constant sources

We take $\sigma = 1$ and the different exact sources $f_{\mathbf{x}_0}$, defined by (33), belong to different subclass $\mathcal{F}_c$. Each subclass $\mathcal{F}_c$ is defined by the fixed known values α, β and R_0 and for all centers $\mathbf{x}_0$ (of the corresponding closed circle U regarding the sources $f_{\mathbf{x}_0}$) are contained in the disk centered at $(0, 0)$ and radius $R - R_0$. As mentioned before, the *inverse problem* consists in finding an approximation of the center $\mathbf{x}_0 = (r_0, \theta_0)$, in polar coordinates, of the corresponding closed circle U of the source $f_{\mathbf{x}_0}$ with the same values of the radius R_0, α and β,where β is given by (30). The values of parameters α, β and R_0 and the center $\mathbf{x}_0$ that define one source $f_{\mathbf{x}_0}$ in a subclass $\mathcal{F}_c$ are given in Table V.

Table V shows the numerical results for noisy data V_δ on $\partial\Omega$ with three different noise levels $\delta = 0.1$, 0.05 and 0.01. The point where the functional $J_\delta(r, \theta)$ is minimized is denoted by $\mathbf{x}^*_{\delta,n}$, where n is the number of iterations conducted by *fmincon*. The relative errors in the Euclidean norm between $\mathbf{x}_0 = (r_0, \theta_0)$ and $\mathbf{x}^*_{\delta,n} = (r^*_\delta, \theta^*_\delta)_n$ are in the columns of each value of δ. In this case, the relative errors decrease when the error in date V_δ decreases. These results show numerical convergence regarding the noise levels δ. Additionally, the accuracy of the solution in this case is high for the circular regions Ω. Therefore, the numerical results in Table V show that the method proposed here is stable considering the noise in the input data.

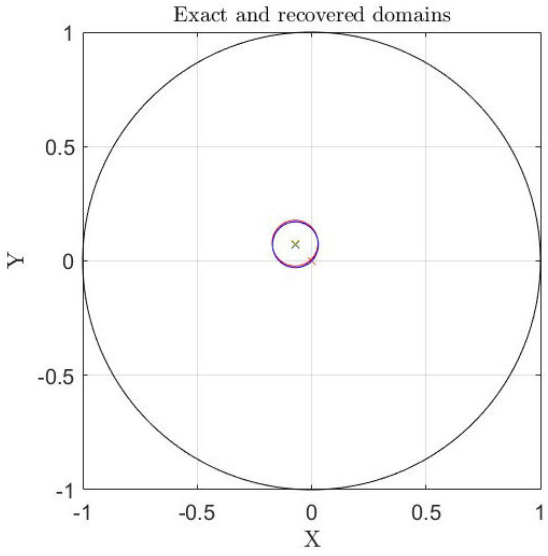

FIGURE 24. Exact and recovered domains of the source $f_{\mathbf{x}_0}$ and its approximate solution $\mathbf{x}^*_{\delta,n}$ at iteration $n = 5$, obtained with the Algorithm 2 given in the Subsec. 7.4, for $\mathbf{x}_0 = (r_0, \theta_0) = (0.1, (3/4)\pi)$, $R_0 = 0.1$, $\alpha = 12$ and $\delta = 0.1$.

TABLE V. Relative errors for different values of δ, R_0, α and β applying Algorithm 2 proposed in Subsec. 7.4 for a circular region Ω, where β is given by (30) and the subscript n is the number of iterations conducted by *fmincon*.

R_0	$\mathbf{x}_0 = (r_0, \theta_0)$	α	$\delta = 0.1$	$\mathbf{x}^*_{\delta,n} = (r^*_\delta, \theta^*_\delta)_n$	$\delta = 0.05$	$\mathbf{x}^*_{\delta,n} = (r^*_\delta, \theta^*_\delta)_n$	$\delta = 0.01$	$\mathbf{x}^*_{\delta,n} = (r^*_\delta, \theta^*_\delta)_n$
0.2	$(0.5, \frac{5}{4}\pi)$	10	0.0285	$(0.5038, 3.8996)_5$	0.0204	$(0.4942, 3.9439)_5$	0.0151	$(0.4993, 3.9120)_5$
0.1	$(0.5, \frac{5}{4}\pi)$	6	0.0394	$(0.4831, 3.9476)_5$	0.0214	$(0.4957, 3.9466)_5$	0.0139	$(0.5015, 3.9405)_5$
0.1	$(0.3, \frac{3}{4}\pi)$	9	0.0567	$(0.3152, 2.3314)_5$	0.0320	$(0.3065, 2.3328)_5$	0.0174	$(0.3036, 2.3439)_5$
0.1	$(0.1, \frac{3}{4}\pi)$	12	0.0667	$(0.1056, 2.3212)_5$	0.0527	$(0.1034, 2.3955)_5$	0.0405	$(0.1040, 2.3604)_5$
0.1	$(0.6, \frac{1}{6}\pi)$	8	0.0337	$(0.5881, 0.5512)_5$	0.0265	$(0.6109, 0.5427)_5$	0.0123	$(0.5996, 0.5358)_5$
0.1	$(0.1, \frac{1}{6}\pi)$	7	0.0523	$(0.1042, 0.4930)_5$	0.0503	$(0.1049, 0.5325)_5$	0.0477	$(0.1043, 0.5435)_5$

Figure 22 shows the noisy data V_δ (blue), for $\delta = 0.1$, generated by the function *random* of MATLAB, Fig. 23 shows the recovered harmonic source $h_{\alpha(\delta)}$ obtained with Algorithm 2 (proposed in Subsec. 7.4) at iteration $n = 5$. Finally, Fig. 24 shows the recovered domain U, with center $\mathbf{x}^*_{\delta,n}$, corresponding to the recovered source $f_{\mathbf{x}^*_{\delta,n}}$ obtained with this algorithm. The last figure shows that the recovered domain U, with center $\mathbf{x}^*_{\delta,n}$ obtained with the method proposed in this work is indistinguishable. The corresponding figures for the other values of the parameters α, β, R_0, $\mathbf{x}_0$ and δ are qualitatively similar and are not included.

8. Conclusions

An elliptic boundary value problem is used to study the forward and inverse source problems. The inverse problem has a unique solution when the space of harmonic functions is considered. This work presents a stable algorithm for recovering that harmonic function. The solution to the boundary value problem is obtained using circular harmonics.

The Tikhonov regularization method is employed to get the algorithm. This method carries up to one variant of the normal equation. In addition to the Tikhonov regularization parameter, we consider another regularization parameter, which is obtained by truncating the series that gives the solution of the normal equations. Thus, the algorithm considers two regularization parameters. The numerical results show the feasibility of the proposed algorithm. The work also considers the problem of determining the irradiance using the Irradiance Transport Equation for the case in which that equation can be written as a Poisson equation with a null Neumann boundary condition, and the source is a harmonic function. When the source is not harmonic, we can consider additional information to get the uniqueness of the inverse problem. This additional information can be obtained from the experts in the area where the problem is studied. To get the whole source, an additional minimization problem must be defined. To illustrate this, we consider one case for the non harmonic function in which the source belongs to a particular class of piecewise constant sources.

Appendix

A. Series calculations

To solve problem (1), we consider that the function f can be expanded in the form

$$f(r,\theta) = \sum_{k=1}^{\infty} f_k^1 A_k r^k \cos k\theta + f_k^2 A_k r^k \sin k\theta,$$

where A_k is a normalization factor. To calculate A_k, we have to calculate the norm of $r^k \cos k\theta$ and $r^k \sin k\theta$:

$$\left\|r^k \sin k\theta\right\|^2_{L_2(\Omega)} = \left\|r^k \cos k\theta\right\|^2_{L_2(\Omega)} = \int_0^R \int_0^{2\pi} (r^k \cos k\theta)^2 r dr d\theta = \int_0^R r^{2k+1} dr \int_0^{2\pi} \cos^2 k\theta d\theta = \frac{R^{2k+2}}{2k+2}\pi,$$

then $\left\|r^k \cos k\theta\right\|_{L_2(\Omega)} = \sqrt{[R^{2k+2}/(2k+2)]\pi}$. Hence

$$\frac{r^k \cos k\theta}{\|r^k \cos k\theta\|} = \frac{\sqrt{2k+2}}{\sqrt{R^{2k+2}}\sqrt{\pi}} r^k \cos k\theta = \frac{\sqrt{2k+2}}{\sqrt{\left(R^{k+1}\right)^2}\sqrt{\pi}} r^k \cos k\theta = \frac{\sqrt{2k+2}}{R^{k+1}\sqrt{\pi}} r^k \cos k\theta.$$

So, we have

$$\frac{\sqrt{2k+2}}{R^{k+1}\sqrt{\pi}}r^k\cos k\theta = A_k r^k\cos k\theta,$$

from where

$$A_k = \frac{\sqrt{2k+2}}{R^{k+1}\sqrt{\pi}}. \tag{A.1}$$

We do the same for the biharmonic function

$$u(r,\theta) = \sum_{k=1}^{\infty} a_k A_k r^k\cos k\theta + b_k A_k r^k \sin k\theta + \sum_{k=1}^{\infty} c_k B_k r^{k+2}\cos k\theta + d_k B_k r^{k+2}\sin k\theta. \tag{A.2}$$

We calculate the norm of $r^{k+2}\cos k\theta$ to obtain the orthonormal basis

$$\left\|r^{k+2}\cos k\theta\right\|^2 = \int_0^R\int_0^{2\pi}(r^{k+2}\cos k\theta)^2 r dr d\theta = \int_0^R r^{2(k+2)+1}dr\int_0^{2\pi}\cos^2 k\theta d\theta = \frac{R^{2k+6}}{2k+6}\pi,$$

then $\left\|r^{k+2}\cos k\theta\right\| = \sqrt{[R^{2k+6}/(2k+6)]\pi}$. Hence

$$\frac{r^{k+2}\cos k\theta}{\|r^{k+2}\cos k\theta\|} = \frac{\sqrt{2k+6}}{\sqrt{R^{2(k+3)}}\sqrt{\pi}}r^{k+2}\cos k\theta = \frac{\sqrt{2k+6}}{R^{k+3}\sqrt{\pi}}r^{k+2}\cos k\theta.$$

So, we have

$$\frac{\sqrt{2k+6}}{R^{k+3}\sqrt{\pi}}r^{k+2}\cos k\theta = B_k r^k\cos k\theta \Rightarrow B_k = \frac{\sqrt{2k+6}}{R^{k+3}\sqrt{\pi}}.$$

Remember that the Laplace operator in polar coordinates is defined by

$$\Delta_{(r,\theta)}f = \frac{1}{r}\frac{\partial}{\partial r}\left(r\frac{\partial f}{\partial r}\right) + \frac{1}{r^2}\frac{\partial^2 f}{\partial\theta^2} = \frac{1}{r}\frac{\partial f}{\partial r} + \frac{\partial^2 f}{\partial r^2} + \frac{1}{r^2}\frac{\partial^2 f}{\partial\theta^2}.$$

Applying $\Delta_{(r,\theta)}$ to (A.2)

$$\Delta_{(r,\theta)}(r^{k+2}\cos k\theta) = \frac{\partial^2(r^{k+2}\cos k\theta)}{\partial r^2} + \frac{1}{r}\frac{\partial(r^{k+2}\cos k\theta)}{\partial r} + \frac{1}{r^2}\frac{\partial^2(r^{k+2}\cos k\theta)}{\partial\theta^2} = [(k+2)(k+1)]r^k\cos k\theta$$
$$+ (k+2)r^k\cos k\theta - k^2 r^k\cos k\theta = (4k+4)r^k\cos k\theta.$$

So,

$$\Delta_{(r,\theta)}u(r,\theta) = \sum_{k=1}^{\infty} c_k B_k(4k+4)r^k\cos k\theta + d_k B_k(4k+4)r^k\sin k\theta = \sum_{k=1}^{\infty} f_k^1 A_k r^k\cos k\theta + f_k^2 A_k r^k\sin k\theta.$$

Thus

$$c_k = \frac{A_k}{4B_k(k+1)}f_k^1, \qquad d_k = \frac{A_k}{4B_k(k+1)}f_k^2.$$

On the other hand

$$\frac{\partial}{\partial r}u(r,\theta) = \sum_{k=1}^{\infty} kA_k r^{k-1}\left(a_k\cos k\theta + b_k\sin k\theta\right) + \sum_{k=1}^{\infty}(k+2)B_k r^{k+1}\left(c_k\cos k\theta + d_k\sin k\theta\right).$$

So,

$$\frac{\partial}{\partial r}u(R,\theta) = \sum_{k=1}^{\infty}\left(ka_k A_k R^{k-1} + (k+2)c_k B_k R^{k+1}\right)\cos k\theta + \left(kb_k A_k R^{k-1} + (k+2)d_k B_k R^{k+1}\right)\sin k\theta.$$

Thus,

$$ka_kA_kR^{k-1} + (k+2)c_kB_kR^{k+1} = 0.$$

Then,

$$a_k = -\frac{(k+2)c_kB_kR^{k+1}}{kA_kR^{k-1}} = -\frac{(k+2)c_kB_kR^2}{kA_k} = -\frac{(k+2)B_kR^2A_k}{4B_k(k+1)kA_k}f_k^1 = -\frac{(k+2)R^2}{4(k+1)k}f_k^1.$$

Analogously

$$b_k = -\frac{(k+2)R^2}{4(k+1)k}f_k^2.$$

B. Trace of a function

Let Ω be a bounded domain in $\mathbb{R}^n$, and let S be an $(n-1)$-dimensional surface that belongs to $\overline{\Omega}$, for example, $S = \partial\Omega$. We will call the trace $f|_S$ of the function $f \in C(\overline{\Omega})$ on S the value that the continuous function f takes on this surface S, *i.e.*, by the trace of a continuous function on S we mean its value extended uniquely according to the continuity on S. In this case, the trace coincides with the restriction of the function f on the surface S. The concept of the trace of a function on S can also be introduced for functions in $H^1(\Omega)$. By definition, $H^1(\Omega)$ is the completion of the space $C^1(\overline{\Omega})$, endowed with the norm

$$||f||_{H^1(\Omega)} = \|f\|_{L_2(\Omega)} + \|D^1f\|_{L_2(\Omega)}, \tag{B.1}$$

where D^1f denotes the vector whose entries are given by: $D_i^1f = \partial f/\partial x_i$, $i = 1, 2, ..., n$. Here, D_i^1f is the generalized derivative of order one of the function f corresponding to the independent variable x_i, and D^1 is called the operator of generalized first derivatives. The definition of the generalized derivative of order one D_i^1u of the function u corresponding to independent variable x_i, $i = 1, 2, ..., n$, is given by the following [10] p. 126:

Definition 2. (First generalized derivative) *The function $v \in L_{2,loc}(\Omega)$ is called the first generalized derivative (or generalized derivative of order one) of the function $u \in L_{2,loc}(\Omega)$, which is denoted by $v = D_i^1u$ corresponding to independent variable x_i, $i = 1, 2, ..., n$, if the following equality holds:*

$$\int_\Omega v\varphi d\Omega = -\int_\Omega uD_i^1\varphi d\Omega, \tag{B.2}$$

for all $\varphi \in {C_0}^\infty(\Omega)$, where $L_{2,loc}(\Omega) = \{v : \Omega' \to \mathbb{R} \mid$ for all $\Omega' \Subset \Omega$ and $\int_{\Omega'} f^2d\Omega < \infty\}$, here the symbol $\Subset$ indicates strict containment, and ${C_0}^1(\Omega)$ is the set of functions which take the value zero on the boundary $\partial\Omega$ of the bounded domain Ω.

The function v that satisfies the relation (B.2) is unique; the proof can be found in [10].

Then, for $f \in H^1(\Omega)$, there exists a sequence of functions f_p, $p = 1, 2, ...$, from $C^1(\overline{\Omega})$ that converges to f in $H^1(\Omega)$. For each function $(f_p - f_q)$, $p, q = 1, 2, ...$, the inequality holds

$$\|f_p - f_q\|_{L_2(S)} \leq C\,\|f_p - f_q\|_{H^1(\Omega)},$$

where $C > 0$ is a constant that does not depend of the function $(f_p - f_q)$.

Since $\|f_p - f_q\|_{H^1(\Omega)} \to 0$ as $p, q \to \infty$, we also have $\|f_p - f_q\|_{L_2(S)} \to 0$ as $p, q \to \infty$. This means that the sequence of the traces of the functions f_p on S is Cauchy sequence in $L_2(S)$. Furthermore, since $L_2(S)$ is complete, there exists a function $f_S(x) \in L_2(S)$ such that the sequence of traces $f_p|_S$ converges to it as $p \to \infty$. Taking the limit in the previous inequality, we obtain

$$\|f_p - f_S\|_{L_2(S)} \leq C\,\|f_p - f\|_{H^1(\Omega)}.$$

Now, let us see that the function f_S does not depend on how the sequence f_p, $p = 1, 2, ...$, is chosen, which approximates the function f in the norm from $H^1(\Omega)$. Indeed, let $\widetilde{f}_k$, $k = 1, 2, ...$, be another sequence of functions in $C^1(\overline{\Omega})$ for which $\left\|f - \widetilde{f}_k\right\|_{H^1(\Omega)} \to 0$ as $k \to \infty$, and let $\widetilde{f}_S(x)$ be the limit in the norm from $L_2(S)$ of the sequence $\widetilde{f}_k|_S$, $k = 1, 2, ...$

Then, from the previous inequalities, we have that

$$\left\|\widetilde{f}_S - f_S\right\|_{L_2(S)} \leq \|f_S - f_q\|_{L_2(S)} + \left\|\widetilde{f}_q - f_q\right\|_{L_2(S)} + \left\|\widetilde{f}_S - \widetilde{f}_q\right\|_{L_2(S)} \leq C\left(\|f_q - f\|_{H^1(\Omega)} + \left\|f_q - \widetilde{f}_q\right\|_{H^1(\Omega)} + \left\|\widetilde{f}_q - \widetilde{f}_S\right\|_{H^1(\Omega)}\right).$$

The last expression of the last inequality tends to zero as $q \to \infty$, we have $f_S = \widetilde{f}_S$.

Thus, the concept of the trace of a function has been determined for any element f of $H^1(\Omega)$. Therefore, we have the following definition:

Definition 3. *The function $f_S \in L_2(S)$ is called the trace of the function f in $H^1(\Omega)$ on the surface S, and it is denoted by the symbol $f|_S$. The norm $\|f|_S\|_{L_2(S)}$ is denoted by $\|f\|_{L_2(S)}$.*

This concept is indeed a generalization of the concept of the value of a function on an $(n-1)$-dimensional surface, that is, of the restriction of a continuous function f to a surface S. This allows us to define the operator trace, denoted by tr as follows: $tr : H^1(\Omega) \to L_2(S)$ such that $tr(f) = f|_S$.

C. On correctness of the Algorithms 1 and 2

For the Tikhonov regularization, the following Theorem can be found in Ref. [1], p. 39.

Theorem 7. *Let $K : X \to Y$ be a linear, compact, and injective operator and $\alpha > 0$ and $x^* \in X$ be the exact solution of $Kx^* = y^*$. Furthermore, let $y^\delta \in Y$ with $\|y^\delta - y^*\|_Y \leq \delta$. Then*

a) Let $x^* = K^*z \in R(K^*)$ with $\|z\|_Y \leq E$. We choose $\alpha(\delta) = c\delta/E$ for some $c > 0$. Then the following estimates hold:

$$\left\|x^{\alpha(\delta),\delta} - x^*\right\|_X \leq \frac{1}{2}(1/\sqrt{c} + \sqrt{c})\sqrt{\delta E}, \tag{C.1}$$

$$\left\|Kx^{\alpha(\delta),\delta} - y^*\right\|_X \leq (1+c)\delta. \tag{C.2}$$

b) For some $\sigma \in (0, 2]$, let $x^* = (K^*K)^{\sigma/2}z \in R((K^*K)^{\sigma/2})$ with $\|z\|_X \leq E$. The choice $\alpha(\delta) = c(\delta/E)^{2/(\sigma+1)}$ for $c > 0$ leads to the error estimates

$$\left\|x^{\alpha,\delta} - x^*\right\|_X \leq H\delta^{\sigma/(\sigma+1)}E^{1/(\sigma+1)}, \tag{C.3}$$

$$\left\|Kx^{\alpha,\delta} - y^*\right\|_X \leq (1 + c_{\sigma+1}c^{(\sigma+1)/2})\delta, \tag{C.4}$$

where $H = (1/2\sqrt{c}) + c_\sigma c^{\sigma/2}$. Here, c_σ are the constants for the choice of q of the part (a) of Theorem 2.8 [1], p. 35. Therefore, for $\sigma \leq 2$ Thikonov's regularization method is optimal for the information $\|(K^*)^{-1}x^*\|_Y \leq E$ or $\|(K^*K)^{-\sigma/2}x^*\|_X \leq E$, respectively (provided K^* is one-to-one).

Now, we get an estimate for the truncated series

$$\begin{aligned}\left\|f - f^N_{\alpha(\delta)}\right\|_{L_2(\Omega)} &\leq \left\|f - f_{\alpha(\delta)} + f_{\alpha(\delta)} - f^N_{\alpha(\delta)}\right\|_{L_2(\Omega)} \leq \left\|f - f_{\alpha(\delta)}\right\|_{L_2(\Omega)} + \left\|f_{\alpha(\delta)} - f^N_{\alpha(\delta)}\right\|_{L_2(\Omega)} \\ &= \left\|f - f_{\alpha(\delta)}\right\|_{L_2(\Omega)} + \sqrt{\sum_{k=N+1}^{\infty}\left(f^1_{k,\alpha(\delta)}\right)^2 + \left(f^2_{k,\alpha(\delta)}\right)^2},\end{aligned}$$

where $f^N_{\alpha(\delta)}$ is the approximated truncated source of $f_{\alpha(\delta)}$, and $f^1_{k,\alpha(\delta)}$, $f^2_{k,\alpha(\delta)}$ are the Fourier coefficients of the approximated source $f_{\alpha(\delta)}$, which are given by

$$f^i_{k,\alpha(\delta)} = \overline{A}_k A_k V^i_{k,\delta},\ i = 1, 2, \tag{C.5}$$

where $V^{i,\delta}_k, i = 1, 2$ are the Fourier coefficients of the error measurement V_δ, with $\|V - V_\delta\|_{L_2(\Omega)} \leq \delta$, and $\overline{A}_k$ is given in Eq. (18). Taking into account the coefficients A_k, E_k, Φ_k and $\overline{A}_k$ given in Sec. 3, we have $\Phi_k = \Gamma_k A_k R^k + \Lambda_k B_k R^{k+2} = -\sqrt{2}R\sqrt{k+1}/4\sqrt{\pi}$ and

$$\overline{A}_k A_k = \frac{E_k A_k}{\sqrt{\pi}E_k\Phi_k - \alpha} = \frac{-4}{\sqrt{\pi}R^{k-1}[R^3 + 4k\alpha]}, \tag{C.6}$$

where

$$\frac{1}{(R^3 + 4k\alpha)} \leq 1,$$

for the values suggested in this work $\alpha = 10^{-5}$, $k = 16$ and $R \geq 1$. Then

$$(\overline{A}_k A_k)^2 \leq \frac{16}{\pi}.$$

Therefore,

$$\left\|f-f_{\alpha(\delta)}^{N}\right\|_{L_2(\Omega)} \leq \left\|f-f_{\alpha(\delta)}\right\|_{L_2(\Omega)} + \sqrt{\sum_{k=N+1}^{\infty}\left(\overline{A}_k A_k V_{k,\delta}^1\right)^2 + \left(\overline{A}_k A_k V_{k,\delta}^2\right)^2} = \left\|f-f_{\alpha(\delta)}\right\|_{L_2(\Omega)}$$

$$+ \sqrt{\sum_{k=N+1}^{\infty}\left(\overline{A}_k A_k\right)^2\left[\left(V_{k,\delta}^1\right)^2 + \left(V_{k,\delta}^2\right)^2\right]} \leq \left\|f-f_{\alpha(\delta)}\right\|_{L_2(\Omega)} + \frac{4}{\sqrt{\pi}}\sqrt{\sum_{k=N+1}^{\infty}\left[\left(V_{k,\delta}^1\right)^2 + \left(V_{k,\delta}^2\right)^2\right]}$$

$$= \left\|f-f_{\alpha(\delta)}\right\|_{L_2(\Omega)} + \frac{4\left\|V_\delta\right\|_{L_2(\Omega)}}{\sqrt{\pi}} \leq \left\|f-f_{\alpha(\delta)}\right\|_{L_2(\Omega)} + \frac{4\delta}{\sqrt{\pi}},$$

where $\left\|f-f_{\alpha(\delta)}\right\|_{L_2(\Omega)} \to 0$ since Tikhonov regularization is an admissible strategy (see Theorem 4). Clearly, $(4\delta/\sqrt{\pi}) \to 0$, when $\delta \to 0$.

These results show the mathematical correctness of the algorithms 1 and 2. Furthermore, the accuracy of the Tikhonov regularization method is at least of order one or linear if we have a priori information about the exact source f (see Theorem 7).

D. Inverse operator and numerical instability

A linear operator $A : X \to Y$, where X and Y are Hilbert spaces, is continuous in a point $x \in X$ if and only if it is continuous in every point of X. From this, when an operator is not continuous, it is not continuous at each point of the space X. This is reflected when we solve operational equations of the form $Ax = y$. One way to proceed consists of discretization of that operational equation to get a system of linear equations $A_N x_N = y_N$, where A_N, x_N, and y_N are discretization of the A, x, and y, respectively. The operators $A_N \to A$ when the following norm is consider $\|A\| = sup_{\|x\|\neq 0}\{\|Ax|/\|x\|\}$. However, the operators A_n^{-1} do not converge to A^{-1}. Furthermore, the matrices that represent the operator A_N (we can use the same symbol for the matrix representation and the operators) are ill-conditioned, which produces large changes in the sought solution when small errors appear on the right side of the equation. Examples can be found in Ref. [1], p. 11, and Ref. [19], p. 6. Note that the errors in the right hand of the operational equation appear as errors in the right hand on the linear system of equations. Thus, the non-continuity of one operator A^{-1} can be interpreted as follows: the images of close points may be very far from each other, which can be related to the ill-conditioning of the matrices A_N. Notably, the operator A is linear, compact, and injective, and x and y belong to appropriate Hilbert spaces of infinite dimension, which implies that A^{-1} is not continuous. This kind of operator appears in many applications [19].

In this work, the operators A_N and A_N^{-1} are given by

$$A_N(f)(\theta) = \sum_{k=1}^{N} C_k \frac{\cos(k\theta)}{\sqrt{\pi}} + D_k \frac{\sin(k\theta)}{\sqrt{\pi}},$$

$$A_N^{-1}(V_\delta)(\theta) = \sum_{k=1}^{N} \frac{4Rk\sqrt{k+1}}{\sqrt{2}[k-R^2(k+2)]}\left[V_{k,\delta}^1 \frac{\cos(k\theta)}{\sqrt{\pi}} + V_{k,\delta}^2 \frac{\sin(k\theta)}{\sqrt{\pi}}\right],$$

where we can see that

$$f_{k,\delta}^i = \frac{4Rk\sqrt{k+1}}{\sqrt{2}[k-R^2(k+2)]} V_{k,\delta}^i$$

and

$$\frac{\sqrt{2}k|V_{k,\delta}^i|}{R} \leq |f_{k,\delta}^i|, \tag{D.1}$$

for $i = 1, 2$, then $|f_{k,\delta}^i| \to \infty$, when $k \to \infty$ by (D.1). These results show the numerical instability of the inverse of the operator A defined in Eq. (12).

1. A. Kirsch, An Introduction to the Mathematical Theory of Inverse Problems, 2nd ed. (Springer New York, NY, 2011), pp. 23-61.
2. J-C. Liu, *An inverse source problem of the Poisson equation with Cauchy data*, Electr. J. Differ. Equ. **2017** (2017).
3. A. Benyoucef, L. Alem, and L. Chorfi, *Numerical method for solving inverse source problem for Poisson equation*, Asian-Eur. J. Math. **14** (2021), https://doi.org/10.1142/S1793557121501734
4. A. Badia and T. Duong, *Some remarks on the problem of source identification from boundary measurements*, Inverse Probl. **14** (1998) 883, https://iopscience.iop.org/article/10.1088/0266-5611/14/4/008
5. J. Conde, C. Hernández, M. Morín, J. Oliveros and H. Juárez, *Stable Numerical Identification of Sources in Non-Homogeneous Media*, Mathematics **10** (2022) https://doi.org/10.3390/math10152726
6. M. Morín, C. Netzahualcoyotl, J. Oliveros, J. Conde and H. Juárez, *Stable identification of sources located on separation interfaces of two different homogeneous media*, Adv. Differ. Equ. Contr. **20** (2019) 53, http://dx.doi.org/10.17654/DE020010053
7. A. Fraguela, J. Oliveros, M. Castillo and J. Conde, *Identification of piecewise constant sources in non-homogeneous media based on boundary measurements*. Appl. Math. Model., **39** (2015), 7697, https://doi.org/10.1016/j.apm.2015.04.026
8. A. Martinez, M. Rodriguez, F. Campos, A. Granados and C. Vargas, *Aberration patterns in the optical testing surfaces using transport of intensity equation*, Rev. Mex. Fis., **68** (2022) 1, https://doi.org/10.31349/RevMexFis.68.011301
9. R. Adams, and J. Fournier, Sobolev spaces, 2nd ed. (Academic Press, Oxford, 2003), pp. 23-61.
10. V. Mikhailov, Partial diferential equations. (MIR Publishers, 1978), pp. 101-161.
11. A. Fraguela, M. Morin and J. Oliveros, *Inverse electroencephalography for volumetric sources*, Math. Comput. Simulat. **78** (2008) 481, https://doi.org/10.1016/j.matcom.2007.06.010
12. D. Luenberger, Optimization by vector space methods. (John Wiley & Sons, NY, 1969).
13. A. Tikhonov, A. Goncharsky, V. Stepanov, and A. Yagola, Numerical Methods for the Solution of ill-Posed Problems, 2nd ed. (Springer Nauka, Moscow, 1995).
14. P. Hansen, The L-curve and its use in the numerical treatment of inverse problems, Invited chapter in: P. Johnston (Ed.), Computational Inverse Problems in Electrocardiography, (WIT Press, Southampton, 2001), pp. 119-142.
15. P. Soltani, A. Moradi, A. Darudi, and R. Shomali, *High-resolution optical surface testing using transport of intensity equation*, Proc. SPIE - Int. Soc. Opt. Eng. **8785** (2013), https://doi.org/10.1117/12.2026289
16. M. Campos and R. Diaz, *Irradiance transport equation from geometrical optics considerations*, Rev. Mex. Fis., **52** (2006) 546,
17. M. Reed, *Deterministic phase retrieval: a Green's function solution*. J. Opt. Soc. Am. **73** (1983) 1434, https://doi.org/10.1364/JOSA.73.001434
18. R. Shomali, A. Darudi, and S. Nasiri, *Application of irradiance transport equation in aspheric surface testing*, Optik, **123** (2012) 1282, https://doi.org/10.1016/j.ijleo.2011.08.009
19. I. Algredo-Badillo, J.J. Conde-Mones, C.A. Hernández-Gracidas, M.M. Morín-Castillo, J.J. Oliveros-Oliveros and C. Feregrino-Uribe. *An FPGA-based analysis of trade-offs in the presence of ill-conditioning and different precision levels in computations*, PloS One, **15** (2020) e0234293. https://doi.org/10.1371/journal.pone.0234293
20. S. Roman, Advanced linear algebra, 2nd ed. (New York: Springer, 2005), pp. 75-80.
21. W. Rudin, Functional analysis, 2nd ed. International Series in Pure and Applied Mathematics (New York, McGraw-Hill, Inc., 1991).